Ultrafast Melting of a Charge-Density Wave in the Mott Insulator 1T-TaS$_2$

S. Hellmann,[1] M. Beye,[2,*] C. Sohrt,[1] T. Rohwer,[1] F. Sorgenfrei,[2] H. Redlin,[4] M. Kalläne,[1] M. Marczynski-Bühlow,[1]
F. Hennies,[3] M. Bauer,[1] A. Föhlisch,[2,†] L. Kipp,[1] W. Wurth,[2] and K. Rossnagel[1,‡]

[1]*Institute for Experimental and Applied Physics, University of Kiel, 24098 Kiel, Germany*
[2]*Institute for Experimental Physics and Centre for Free-Electron Laser Science, University of Hamburg,
22761 Hamburg, Germany*
[3]*MAX-lab, Lund University, Lund, Sweden*
[4]*Deutsches Elektronen-Synchrotron, DESY, 22607 Hamburg, Germany*
(Received 23 April 2010; published 27 October 2010)

Femtosecond time-resolved core-level photoemission spectroscopy with a free-electron laser is used to
measure the atomic-site specific charge-order dynamics of the charge-density wave in the Mott insulator
1T-TaS$_2$. After strong photoexcitation, a prompt loss of charge order and subsequent fast equilibration
dynamics of the electron-lattice system are observed. On the time scale of electron-phonon thermaliza-
tion, about 1 ps, the system is driven across a phase transition from a long-range charge ordered state to a
quasiequilibrium state with domainlike short-range charge and lattice order. The experiment opens the
way to study the nonequilibrium dynamics of condensed matter systems with full elemental, chemical,
and atomic-site selectivity.

Femtosecond time-resolved spectroscopy has become a
powerful tool in condensed matter research because it
delivers direct dynamical information at the fundamental
time scale of elementary electronic processes [1,2]. The
method is particularly useful for complex materials, in
which two or more of the lattice, charge, spin, and orbital
degrees of freedom are strongly coupled. It allows us to
determine the nature and strength of the interactions
between the degrees of freedom, to identify the dominant
interactions, and thus to gain important insights into
ground-state properties, thermally driven phase transitions,
and, possibly, novel hidden phases [3–6].

An exceedingly fertile ground for the combination of
spectral selectivity and femtosecond time resolution has
been found in materials, in which the charge and lattice
degrees of freedom interact strongly to form a coupled
charge-density-wave (CDW)–periodic-lattice-distortion
(PLD) ground state. The quasiparticle and collective
mode dynamics of the CDW-PLD state, the finite
electron-lattice coupling time, and the collapse of the
electronic gap under strong excitation are now known
[4–9]. Yet, direct dynamical information on the CDW
itself, i.e., on the local charge order, is missing. Speci-
fically, it is not clear how fast a CDW can melt and
recondense after impulsive excitation. The present study
provides this fundamental piece of information for the
layered reference compound 1T-TaS$_2$ [4,8–11].

Employing time-resolved x-ray photoemission spectros-
copy (TR-XPS) with a free-electron laser [12,13], we
directly measure the melting of a large-amplitude CDW
in 1T-TaS$_2$ at atomic sites in real time. Our results show
that long-range charge order collapses promptly after
strong optical excitation and that a domainlike quasiequi-

librium CDW-PLD state is reached with a subpicosecond
time constant.

The model system 1T-TaS$_2$ is a complex material with
a simple basic structure consisting of S-Ta-S sandwiches
in which each Ta atom is octahedrally coordinated by six
S atoms. The interesting physics in this compound is
restricted to the hexagonal Ta layers and results from
simultaneously strong electron-phonon and electron-
electron interactions. The phase diagram includes a high-
temperature metallic phase, incommensurate CDW, and
nearly commensurate CDW (NCCDW) phases at inter-
mediate temperatures, and ultimately a low-temperature
commensurate CDW (CCDW) phase coexisting with a
Mott insulator phase [Fig. 1(a)] [10,14].

Our focus here is on the CCDW-to-NCCDW transition.
In the CCDW phase, the Ta atoms are grouped into David-
star clusters consisting of two 6-atom rings which contract
towards the central atom [10]. The Ta atoms are displaced
by up to 7% of the in-plane lattice constant [15] and the
accompanying $\sqrt{13} \times \sqrt{13}$ CDW also has a large ampli-
tude, as roughly 0.4 electrons are transferred from each
atom in the outer ring to the inner atoms [Fig. 1(b)] [16]. In
momentum space, there is not one uniform CDW gap
opening up at the Fermi level E_F. Rather, the electronic
states in the partially filled Ta 5d band are regrouped into
submanifolds [16] and the combination of spin-orbit cou-
pling and CDW reconstruction leads to a distinct and
narrow band at E_F that is susceptible to a Mott-Hubbard
transition [17]. Upon going from the CCDW to the
NCCDW phase, the important effect is loss of phase co-
herence. A domain superstructure emerges [18], where the
structure within the domains is that of the CCDW phase
and the domain walls, or discommensurations, form

a supposedly metallic network that suppresses the Mott phase [19].

To study the local dynamics of the charge degree of freedom across the CCDW-NCCDW transition, one needs a local probe sensitive to the amplitude of the CDW as well as to its degree of commensurability and phase coherence. XPS is such a probe, as the spectra of shallow core levels generally reflect the charge distribution at atomic sites. In $1T$-TaS_2 it is the Ta $4f$ binding energy that is particularly sensitive to the local charge density. In the CCDW phase, there are three inequivalent Ta atoms in the unit cell designated as a, b, and c in the ratio 1:6:6 [Fig. 1(b)] so that, as shown in Fig. 1(c), each Ta $4f$ level is split into two well-separated peaks b and c (the a peak is weak and not readily resolved [20]). In this phase the b–c splitting Δ_{CDW} is a direct measure of the CDW amplitude [21]. In the NCCDW phase, on the other hand, the CDW-induced splitting is much less pronounced due to the broken phase coherence. Here Δ_{CDW} predominantly reflects the size of the commensurate domains relative to

the area of the discommensurations [22]. Figure 1(a) demonstrates that Δ_{CDW} can indeed be regarded as an order parameter for the system, as the temperature dependence of Δ_{CDW} [21] mimics the resistivity curve [19,23].

Our TR-XPS measurements of the order parameter Δ_{CDW} were performed at the plane grating monochromator beam line PG2 [24,25] of the free-electron laser at Hamburg (FLASH) [12] in combination with a synchronized optical pump laser [13,26,27]. The $1T$-TaS_2 single crystals [28] were excited by a 120 fs (FWHM) pump pulse with a photon energy of 1.55 eV. The photoelectrons used to probe the state of the system were generated by a delayed FLASH pulse of $\sim$156 eV, corresponding to the third harmonic of the fundamental. The total energy and time resolutions, including instrumental resolutions, space-charge broadening [29], and temporal jitter [27], were 300 meV (FWHM) and 700 fs (FWHM), respectively. All measured kinetic energies were referenced to the Fermi edge of the unpumped system. Starting with $1T$-TaS_2 deep in the CCDW phase ($T = 10$ K), two optical excitation fluences were used, $F_1 = 1.8$ mJ/cm^2 and $F_2 = 2.5$ mJ/cm^2, corresponding to absorbed energy densities of $\sim$120 meV/Ta and $\sim$165 meV/Ta, respectively. These values are close to the electronic band energy gain in the CCDW phase ($\sim$ 160 meV/Ta [17]) and they are larger than the energy density required to heat the excited volume to above the CCDW-NCCDW transition temperature ($\sim$ 110 meV/Ta). We therefore expect photoinduced transitions in the course of which charge *and* lattice order are melting.

Figure 2 shows selected time-resolved Ta $4f$ core-level spectra. Two processes governing the response of the system to the impulsive optical excitation can be readily identified: (i) a subpicosecond reduction of the CDW-induced Ta $4f$ splitting, followed (ii) by a partial
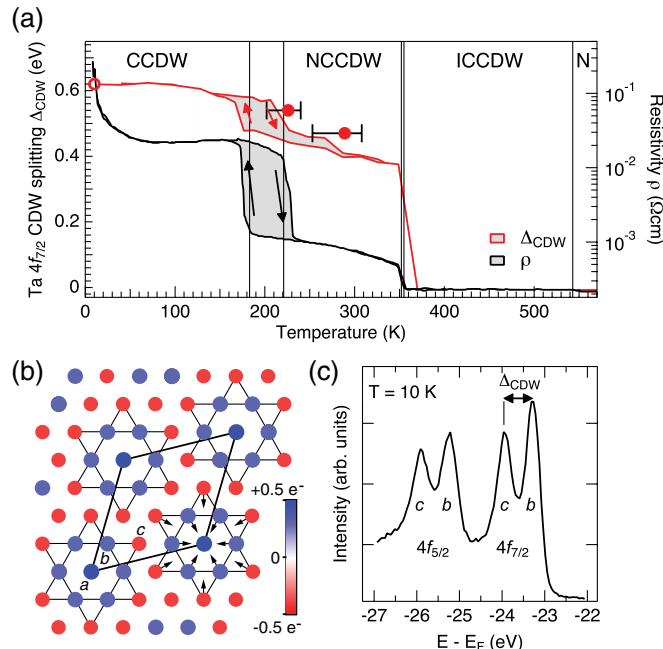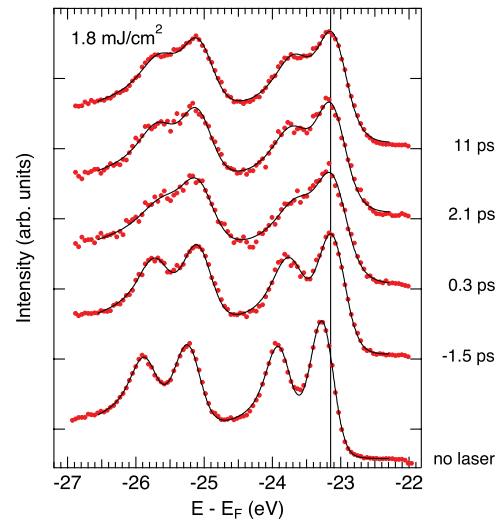

FIG. 1 (color online).   Charge-density-wave phases of $1T$-TaS_2. (a) Phase diagram with the normal undistorted phase (N) as well as incommensurate (IC), nearly commensurate (NC), and commensurate (C) charge-density-wave (CDW) phases. Temperature dependencies of the electrical resistivity (black line, Ref. [19]) and of the CDW-induced Ta $4f$ core-level splitting Δ_{CDW} (red or gray line, Ref. [21], values scaled to match our criterion for Δ_{CDW} [31]) are included. The initial and final Δ_{CDW} values of our pump-probe experiments are indicated by open and filled red or gray circles, respectively. (b) Sketch of the CCDW showing David-star clusters with inequivalent a, b, and c Ta atoms. The arrows indicate the displacement of the Ta atoms from their original positions. The electron density increases towards the center of the cluster. (c) Ta $4f$ photoemission spectrum measured with a photon energy of 156 eV. Each Ta $4f$ level is split into two peaks associated with sites b and c, separated by Δ_{CDW}.

FIG. 2 (color online).   Time-resolved Ta $4f$ photoemission spectra of $1T$-TaS_2 for selected pump-probe delays. Red or gray dots represent the experimental data, solid black curves are fits to the spectra [31], and the vertical line is a guide to the eye illustrating the pump laser induced space-charge shift.

recovery on the picosecond time scale into a quasiequilibrium state with a lifetime of longer than 10 ps. It should be emphasized that both processes are much faster than, and therefore well separated from, the dynamics of the spectral shift and broadening due to the vacuum space charge created by the pump laser (compare the positions of the leading peak in the top four spectra and in the bottom spectrum in Fig. 2).

The ultrafast vaporization and equilibration dynamics shall now be exposed in more detail by analyzing the photoemission intensity map of Fig. 3(a), measured at the lower pump fluence F_1. Note that the effective time resolution of the experiment [700 fs (FWHM)] is directly reflected in the time dependence of the (first-order) Ta $4f_{7/2}$ sideband intensity [Fig. 3(b)], which arises from the absorption of optical laser photons during the ionization process (laser assisted photoelectric effect) [30].

The ultrafast dynamics of the CDW-induced Ta $4f$ splitting is brought to light in Fig. 3(c) which displays the fitted Δ_{CDW} as a function of the pump-probe delay [31]. Within the time resolution of the experiment, Δ_{CDW} drops from the original value of 0.62 eV to 0.47 eV, and it then recovers partially to a quasiequilibrium value $\Delta_{CDW,1}^* = 0.54$ eV with a time constant of ∼900 fs. In contrast to recent valence-band photoemission measurements in the moderate excitation regime [4,8], a periodic modulation of the time-resolved signal cannot be observed. Such modulation is generally caused by the CDW amplitude mode, but is seen to be strongly suppressed in the strong excitation regime, as in our case, because of scattering of the amplitude mode with a high density of excited quasiparticles [4–6,8]. We note that for the higher fluence F_2 the quasiequilibrium Δ_{CDW} value, reached after the initial drop and recovery, is $\Delta_{CDW,2}^* = 0.47$ eV.

The corresponding quasiequilibrium temperature of the electron-lattice system, T^*, can be estimated within the two-temperature model [32]. For the parameters of our experiment [33], we obtain $T_1^* = 226^{+14}_{-24}$ K and $T_2^* = 289^{+19}_{-36}$ K for the two pump fluences used. When plotted in the phase diagram of Fig. 1(a) (filled red or gray circles), the two photoinduced quasiequilibrium states (T_i^*, $\Delta_{CDW,i}^*$) fall, within the error bars, on the equilibrium $\Delta_{CDW}(T)$ curve in the region of the NCCDW phase, thus indicating ultrafast transitions to CDW-PLD states with smaller distortion amplitude and broken phase coherence. For the lower fluence F_1, the calculated time dependence of the electron temperature is shown in Fig. 3(d). The clear anticorrelation with the measured Δ_{CDW} [Fig. 3(c)] suggests that the charge-order parameter is tied to the electron temperature.

We conclude that the observed response of the Ta $4f$ CDW splitting provides strong evidence for the two anticipated melting processes. The impulsive optical excitation causes first a quasi-instantaneous collapse of the charge order by rapidly heating the electrons to a highly elevated temperature and then, when the electrons cool down by transferring their energy to the lattice, a melting of the
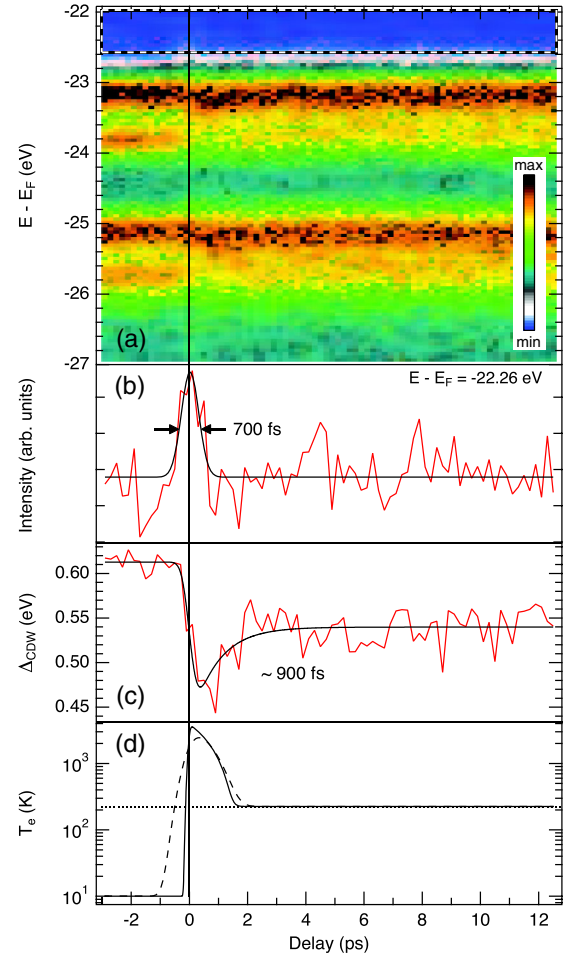

FIG. 3 (color online). Charge-order dynamics in $1T$-TaS$_2$. (a) Time-resolved Ta $4f$ photoemission spectra of $1T$-TaS$_2$ as a function of pump-probe delay, measured at a pump fluence of 1.8 mJ/cm^2. The dashed box centered on -22.26 eV indicates where first-order sideband intensity of the c peak of the Ta $4f_{7/2}$ level is to be expected. (b) Photoemission intensity integrated over the energy interval marked in (a), representing the cross correlation between pump and probe pulses (red or gray curve). The black curve is a Gaussian fit. (c) Ta $4f$ splitting Δ_{CDW} as a function of pump-probe delay (red or gray curve), obtained by line shape fitting [31]. The black curve is a fit to the red or gray curve using a single exponential starting at $t = 0$ convoluted with a Gaussian representing the effective time resolution. (d) Electron temperature T_e as a function of pump-probe delay (solid curve), as calculated from the two-temperature model for the parameters of the experiment [33]. Accounting for the experimental time resolution leads to the dashed curve. The dotted horizontal line marks the equilibrium CCDW-NCCDW transition temperature.

long-range lattice order of the CCDW phase. This scenario implies that the CDW and the PLD, which are so strongly coupled in equilibrium that one cannot exist without the other [37], are decoupled after photoexcitation on the time scale for electron-phonon thermalization [6].

Two more implications of our results are noteworthy. First, the transient collapse of charge order happens on the

same time scale as the collapse of the Mott-Hubbard gap observed in time-resolved valence-band measurements [4,8]. This suggests that the loss of order in the electronic portion of the commensurate CDW-PLD state may be a factor in the ultrafast melting of the Mott phase. Second, the picosecond equilibration time indicates that the CDW-PLD state does not relax into the CCDW domain super-structure of the equilibrium NCCDW phase, which would require the ultrafast nucleation and growth of a (metallic) discommensuration network. It seems more likely that the system relaxes into a state with the same relative size of commensurate and distorted areas, but rather with an in-homogeneous distribution of distorted (metallic) islands in a CCDW background.

In conclusion, strong photoexcitation of the CDW in the Mott insulator $1T$-TaS_2 leads to an ultrafast, temporally decoupled melting of long-range commensurate charge and lattice order: After the prompt collapse of the charge order, the electron-lattice system rapidly equilibrates into a domainlike short-range ordered CDW-PLD phase on the picosecond time scale of electron-phonon thermalization. This result constitutes the first direct measurement of charge-order dynamics in a complex material with com-bined femtosecond resolution and atomic-site sensitivity, thereby establishing the technique of TR-XPS at a free-electron laser. As the time and energy resolution of this element, chemically, and atomic-site selective technique are improving, we can expect many novel insights into the nonequilibrium behavior of condensed matter systems. TR-XPS specifically enables us to create detailed movies of local electron dynamics, not only of ultrafast phase transitions in complex materials but also of chemical re-actions on solid surfaces.

  *Present address: Helmholtz-Zentrum Berlin für Materialien und Energie, Berlin, Germany.
  †Present address: Helmholtz-Zentrum Berlin für Materialien und Energie, Berlin, Germany and Universität Potsdam, Potsdam, Germany.
  ‡rossnagel@physik.uni-kiel.de

 [1] A. L. Cavalieri et al., Nature (London) **449**, 1029 (2007).
 [2] L. Miaja-Avila et al., Phys. Rev. Lett. **101**, 046101 (2008).
 [3] D. J. Hilton et al., J. Phys. Soc. Jpn. **75**, 011006 (2006).
 [4] L. Perfetti et al., Phys. Rev. Lett. **97**, 067402 (2006).
 [5] F. Schmitt et al., Science **321**, 1649 (2008).
 [6] A. Tomeljak et al., Phys. Rev. Lett. **102**, 066404 (2009).
 [7] J. Demsar, K. Biljakovic, and D. Mihailovic, Phys. Rev. Lett. **83**, 800 (1999).
 [8] L. Perfetti et al., New J. Phys. **10**, 053019 (2008).
 [9] J. Demsar et al., Phys. Rev. B **66**, 041101(R) (2002).
[10] P. Fazekas and E. Tosatti, Philos. Mag. B **39**, 229 (1979).
[11] J. K. Freericks et al., Phys. Status Solidi B **246**, 948 (2009).
[12] W. Ackermann et al., Nat. Photon. **1**, 336 (2007).
[13] A. Pietzsch et al., New J. Phys. **10**, 033004 (2008).
[14] S. C. Bayliss, A. M. Ghorayeb, and D. R. P. Guy, J. Phys. C **17**, L533 (1984).
[15] R. Brouwer and F. Jellinek, Physica (Amsterdam) **99B+C**, 51 (1980).
[16] N. V. Smith, S. D. Kevan, and F. J. DiSalvo, J. Phys. C **18**, 3175 (1985).
[17] K. Rossnagel and N. V. Smith, Phys. Rev. B **73**, 073106 (2006).
[18] T. Ishiguro and H. Sato, Phys. Rev. B **44**, 2046 (1991); **52**, 759 (1995).
[19] B. Sipos et al., Nature Mater. **7**, 960 (2008).
[20] H. P. Hughes and J. A. Scarfe, Phys. Rev. Lett. **74**, 3069 (1995).
[21] H. P. Hughes and R. Pollak, Philos. Mag. **34**, 1025 (1976).
[22] F. Zwick et al., Phys. Rev. Lett. **81**, 1058 (1998).
[23] R. Inada, Y. Ōnuki, and S. Tanuma, J. Phys. Soc. Jpn. **52**, 3536 (1983).
[24] M. Martins et al., Rev. Sci. Instrum. **77**, 115108 (2006).
[25] M. Wellhöfer et al., J. Opt. A **9**, 749 (2007).
[26] C. Gahl et al., Nat. Photon. **2**, 165 (2008).
[27] A. Azima et al., Appl. Phys. Lett. **94**, 144102 (2009).
[28] $1T$-TaS_2 single crystals were grown in a temperature gradient of 840–870 °C in 1000 h using iodine vapor transport with excess sulfur (2.5 mg/cm^3) [23].
[29] S. Hellmann et al., Phys. Rev. B **79**, 035402 (2009).
[30] T. Glover et al., Phys. Rev. Lett. **76**, 2468 (1996).
[31] The model function consists of four Doniach-Šunjić lines (plus a linear background) convoluted with a Gaussian. In the fits the Gaussian width from the instrumental resolu-tion, the Ta $4f$ spin-orbit splitting, and the asymmetry parameters were constrained to the known values [20]. The fitted charge-order parameter Δ_{CDW} represents the CDW-induced energy separation between the two Ta $4f$ spin-orbit doublets [one parameter for the two b–c split-tings in Fig. 1(a)].
[32] S. I. Anisimov, B. L. Kapeliovich, and T. L. Perel'man, Sov. Phys. JETP **39**, 375 (1974).
[33] The material specific parameters are the following: elec-tronic heat capacity coefficient $\gamma = 40.3$ J m^{-3} K^{-2} [34], Debye temperature $\Theta_D = 237$ K [35], phonon heat ca-pacity coefficient $\beta = 12.6$ J m^{-3} K^{-4} [35], mass en-hancement parameter $\lambda = 0.85$, reflectivity $R = 0.39$ [36], and absorption coefficient $\alpha = 3 \times 10^7$ m^{-1} [36].
[34] J. A. Wilson, F. J. Di Salvo, and S. Mahajan, Adv. Phys. **24**, 117 (1975).
[35] R. E. Schwall, G. R. Stewart, and T. H. Geballe, J. Low Temp. Phys. **22**, 557 (1976).
[36] A. R. Beal, H. P. Hughes, and W. Y. Liang, J. Phys. C **8**, 4236 (1975).
[37] M. D. Johannes and I. I. Mazin, Phys. Rev. B **77**, 165135 (2008).